Progress In Electromagnetics Research B, Vol. 4, 273–283, 2008

STUDY OF WATER BOLUS EFFECT ON SAR PENETRATION DEPTH AND EFFECTIVE FIELD SIZE FOR LOCAL HYPERTHERMIA

M. A. Ebrahimi-Ganjeh

Communication and Computer Research Center
Ferdowsi University of Mashhad
Iran

A. R. Attari

Electrical Engineering Department
Ferdowsi University of Mashhad
Iran

Abstract—Water bolus is used in microwave hyperthermia of cancer treatment to control the body surface temperature. In this paper the effect of water bolus on SAR distribution is investigated in the muscle layer of a three layered tissue model. Both the SAR penetration depth and the effective field size (EFS) are computed and compared in presence and in absence of the water bolus. Results are provided for distilled and fresh water with three different thicknesses of water bolus. All numerical simulations are performed using the Ansoft HFSS software. Numerical simulation results are in good agreement with published results.

1. INTRODUCTION

Hyperthermia (local, regional, interstitial and whole body) is a therapeutic procedure used to raise the temperature of a region of the body. In cancer treatment it is often used in conjunction with chemotherapy and radiotherapy. Most human tumors have increased blood flow under hyperthermia and hours later. Due to temperature rise, perfusion is increased and increasing the perfusion in the tumor region leads to a higher oxygen concentration. Higher perfusion increases drug delivery for chemotherapy and reoxygenation leads to increasing the efficacy of radiotherapy [1].

Commercially available electromagnetic applicators for local hyperthermia have a typical emitting diameter of 15 cm at a frequency range of 150–430 MHz with therapeutic depth not more than 3 cm. Deep-seated tumors can be heated by arrays of antennas (regional hyperthermia). Several types of applicators have been used clinically, such as waveguide applicators, horn, spiral, current sheet and compact applicator [1].

The water bolus serves the purposes of keeping contact between the microwave applicator and the patient and maintaining controlled temperature of the skin surface. Well controlled coupling of the microwave field from applicator into tissue is necessary for uniform heating and the skin cooling helps prevent overheating of the skin surface, which may cause thermal blisters, or in rare cases, deeper burns in subcutaneous tissue [2].

The temperature increase during the hyperthermia is due to the electromagnetic energy absorption in body tissues. This power absorption is characterized by specific absorption rate (SAR). The SAR quantity is related to the internal E-field by [3]

$$SAR = \frac{\sigma E^2}{\rho} \quad (W/kg) \tag{1}$$

where σ (S/m) is the conductivity of tissue in siemens per meter, ρ is the mass density in kg/m^3 and E is the root mean square (rms) of electric field strength in volts per meter. If the metabolic heating rate, blood flowing cooling rate and the heat losses rate for a tissue have been neglected, the relation between SAR, duration of exposure (dt) and change in temperature (dT) is [3]

$$\frac{dT}{dt} = \frac{SAR}{c} \quad (^\circ C/s) \tag{2}$$

where, c is specific heat capacity (J/kg °C). If we consider the effect of blood flow and metabolic heating rate, the temperature change due to the induced SAR can be obtained by solving the bio-heat equation [4].

Achieving therapeutic temperatures of about 42°C at least in some parts of tumors necessitates SAR of about 20–40 W/kg at the target region [1]. The success of hyperthermia treatment lies in the focalization of the heat inside the cancerous tumor while avoiding this in normal tissues [5]. This focalization of SAR is generally characterized by two parameters named SAR penetration depth and effective field size (EFS).

In local hyperthermia, the EFS is defined as the area that is enclosed within the 50% SAR curve at 1 cm depth inside the tissue

and the penetration depth is defined as the depth at which the SAR becomes $1/e^2$ of its value at the surface [6]. The effects of electromagnetic applicator characteristics e.g., frequency, type and shape on the EFS and SAR penetration depth have been extensively studied in the literature [6–10]. Another subject for investigation is the effect of water bolus on the EFS and SAR penetration depth. It has been shown that the thickness of water bolus is one of the main critical parameters on SAR distribution patterns [11]. The results in [12] show that for Dual Concentric Conductor (DCC) antenna, water bolus thicknesses of 9 mm or greater perturb significantly both the experimental and theoretical SAR distributions.

In this paper, for both the fresh and distilled water and by using a horn applicator for exposure, the effect of water bolus thickness on SAR penetration depth and effective field size (EFS) is investigated at 433 MHz. This investigation is dedicated to local hyperthermia for superficial tumors. A 3-layered tissue model (skin, fat and muscle) is used for numerical simulations. All numerical simulations are performed using the Ansoft HFSS software. Numerical simulation results are in good agreement with published results.

2. BIO-MEDIA AND WATER BOLUS

Biological tissues are modeled by their relative dielectric constant (ε_r) and conductivity. The relative dielectric constant and conductivity of various tissues are frequency-dependent and the values of them over the range of 10 kHz–10 GHz are available at [13, 14].

In local hyperthermia treatments for superficial tumors, applicator is positioned near the body and tumors are often seated near the surface of the body in muscle tissue. So specially in higher frequencies, flat model of the body provides a good accuracy for electromagnetic calculations.

In [7], a 3-layered bio-media (skin, fat and muscle) has been used to study the SAR distribution. The analysis method used in [7] is based on a plane wave spectral technique and the muscle layer is considered to be of infinite thickness. For numerical simulations in this paper the 3-layered model proposed in [7] has been used. The muscle thickness has been assumed to be 15 cm to minimize the numerical reflection from the boundaries. The cross section of the bio-media is also assumed to be $30 \times 30\,\text{cm}^2$ [6]. Dielectric properties, mass densities and thicknesses of different layers of this 3-layered tissue model are shown in Table 1 [7].

For local hyperthermia a thickness of 5–10 mm for water bolus has been used clinically [15]. In this paper water bolus has been filled by distilled and fresh water respectively. The main difference between

fresh and distilled water is their conductivity. Dielectric properties of fresh and distilled water are shown in Table 2. Shell of water bolus is often a thin PVC sheet [16] and can be neglected in calculations.

Table 1. Dielectric properties, mass densities and thicknesses for the 3-layered tissue model at 433 MHz.

	Thickness (mm)	ρ (kg/m^3)	ε_r	σ (S/m)
Skin	**1**	**1130**	**47**	**0.84**
Fat	**5**	**920**	**15**	**0.26**
Muscle	**150**	**1050**	**57**	**1.12**

Table 2. Dielectric properties of water used for filling the water bolus.

	Fresh water	Distilled water
ε_r	**81**	**81**
σ (S/m)	**0.01**	**0.0002**

3. APPLICATOR

Water loading the electromagnetic applicators makes them smaller for focusing [17]. In this paper the water loaded box horn applicator at 433 MHz designed by Gupta [7] is used for exposure. This water loaded box-horn is connected to a WR-229 input waveguide. The frequency range of this waveguide in free space is 3.30–4.90 GHz. Filling a waveguide by a dielectric with relative dielectric constant of ε_r, reduces the operating frequency of the waveguide by a factor of $\sqrt{\varepsilon_r}$. This box-horn is filled with water. The relative dielectric constant and conductivity of the water used by Gupta to fill the applicator are $\varepsilon_r = 78$ and $\sigma = 0.03$. So the frequency range of water loaded WR-229 waveguide is 373 MHz–554 MHz. This applicator is shown in Fig. 1. In Fig. 1, $a = 9.03$ cm, $b = 12.55$ cm, $L = 6.52$ cm and flare angles of the horn exciting the box are 30° in both the E- and H-planes [7].

As shown in Fig. 2, applicator is placed at the center of the front surface of the tissue model. Water bolus is placed between the applicator and the bio-media. Fresh and distilled water (Table 2) have been considered to fill the water bolus. Different thicknesses of water bolus are examined in our numerical simulations (5, 10 and 20 mm). In

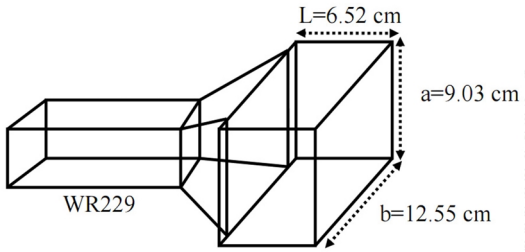

Figure 1. Structure of the applicator [7].

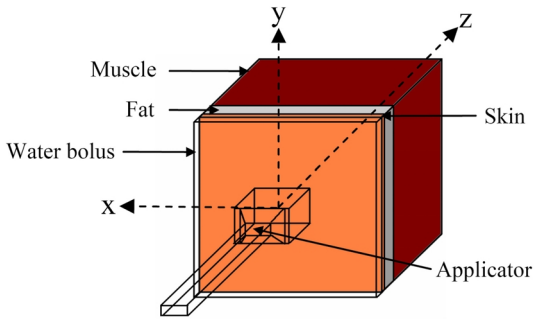

Figure 2. Applicator and three-layered tissue model. Water bolus is placed between the applicator and bio-media.

all simulations there is no space between bio-media, water bolus and applicator.

4. VALIDATION OF NUMERICAL SIMULATIONS

All numerical simulations are performed using the Ansoft HFSS software. To verify the validity of numerical simulations we first perform a validation test and compare its results on the SAR penetration depth with results presented in [7]. In this simulation, the structure shown in Fig. 2 is simulated without water bolus. As shown in Fig. 3, the HFSS results for normalized SAR distribution in fat and muscle layer are in good agreement with the results obtained in [7]. In Fig. 3, the region $z > 6\,\text{mm}$ is corresponding to the muscle layer. All SAR computations in the next sections are presented for muscle layer.

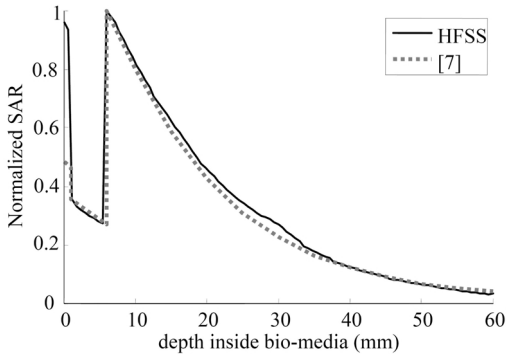

Figure 3. Normalized SAR values without water bolus on the central axis (z-axis) of the 3-layered tissue model.

5. RESULTS ON THE SAR VALUE AND SAR PENETRATION DEPTH INSIDE THE MUSCLE LAYER

In the following, we first compare the maximum induced SAR in the depth of 1 cm inside the muscle layer to investigate which case has better energy coupling. Then, all of the SAR curves are normalized to their maximum values in order to compare the SAR penetration depth and EFS value in different cases.

Table 3. Maximum SAR induced by 1 W output power in depth of 1 cm inside the muscle layer for different water bolus thicknesses.

Thickness	0 mm	5 mm	10 mm	20 mm
Maximum SAR (W/kg) for fresh water	**3.96**	**3.98**	**3.75**	**2.84**
Maximum SAR (W/kg) for distilled water		**4.35**	**4.04**	**2.83**

Table 3 shows the maximum SAR values in depth of 1 cm inside the muscle, induced by the applicator with 1 W output power for various cases. As shown in Table 3, using distilled water for filling the water bolus results in increasing the SAR induced in the muscle layer. Also for both the fresh and distilled water increasing the thickness results in decreasing the induced SAR.

Figures 4 and 5 show the normalized SAR on the central axis of muscle layer for different thicknesses of water bolus filled with distilled

and fresh water respectively. As shown in Figs. 4 and 5, increasing or decreasing the thickness of water bolus does not affect on distribution of the normalized SAR. Therefore the effect of water bolus thickness on the SAR penetration depth can be neglected. Table 4 shows the SAR penetration depth inside the muscle layer for different thicknesses of water bolus filled with distilled or fresh water.

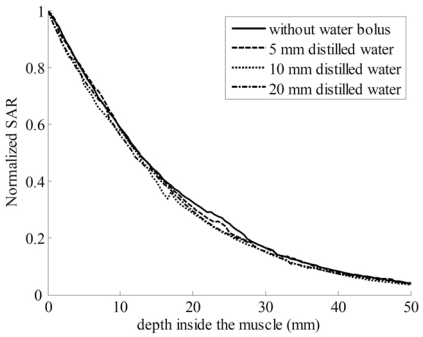

Figure 4. Normalized SAR values for different water bolus thicknesses versus the depth on the central axis of the muscle layer. The water bolus is filled with distilled water.

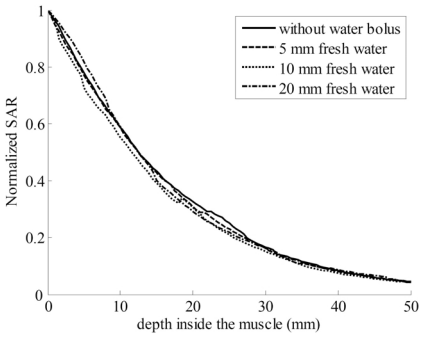

Figure 5. Normalized SAR values for different water bolus thicknesses versus the depth on the central axis of the muscle layer. The water bolus is filled with fresh water.

Table 4. Penetration depth for different water bolus thicknesses.

Thickness	0 mm	5 mm	10 mm	20 mm
Penetration depth (mm) for distilled water	**33**	**33**	**31.5**	**32**
Penetration depth (mm) for fresh water		**32.5**	**32**	**32.5**

6. RESULTS ON THE EFS INSIDE THE MUSCLE LAYER

The effective field size (EFS) is defined as the area that is enclosed within the 50% SAR curve at 1 cm depth inside the muscle layer. Fig. 6(a) depicts the normalized SAR contours of this area for the

water loaded applicator in the case without water bolus. Width of the EFS area for the case without water bolus is 4.5 cm along the x axis and 6.6 cm along the y axis (Fig. 6(b)).

Figure 7 illustrates the normalized SAR contours showing the EFS in depth of 1 cm inside the muscle layer when different values of water bolus thickness are used. These contours are plotted in a 4.5 cm×6.6 cm rectangular box for better comparison. As shown in Fig. 7, for both the fresh and distilled water, by increasing the water bolus thickness, the elliptical contours of the normalized SAR are converted to circular contours which may be more interested in local hyperthermia. Table 5 illustrates the EFS values corresponding to the different cases shown in Figs. 6 and 7.

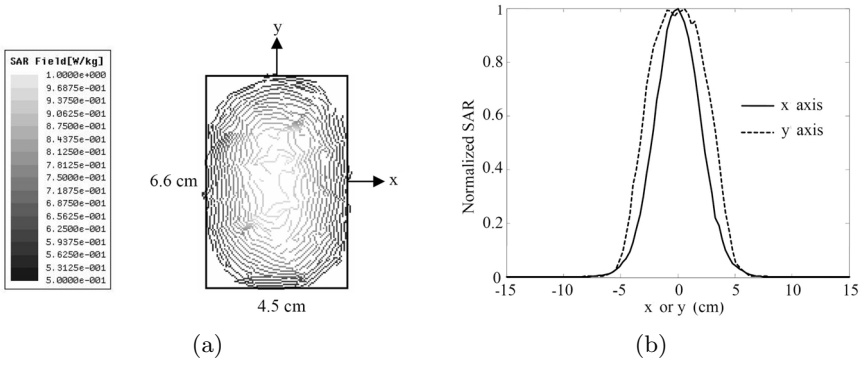

Figure 6. Normalized SAR in the case of without water bolus in depth of 1 cm inside the muscle layer. (a) Contours showing the EFS. (b) Normalized SAR distributions along x and y axis.

Table 5. EFS values for different values of water bolus thickness.

Thickness	0 mm	5 mm	10 mm	20 mm
EFS (cm^2) for fresh water	**25.4**	**22.7**	**20.8**	**22.2**
EFS (cm^2) for distilled water		**21.3**	**18.6**	**21.9**

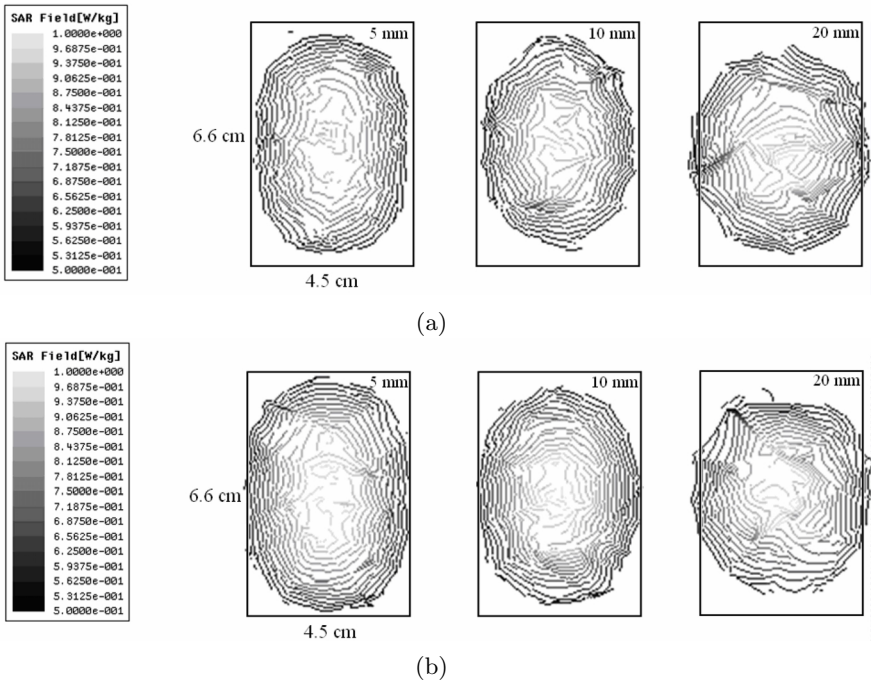

Figure 7. Normalized SAR contours showing the EFS in the presence of water bolus with 5 mm, 10 mm and 20 mm thicknesses. (a) Water bolus filled with distilled water. (b) Water bolus filled with fresh water.

7. CONCLUSIONS

The effect of water bolus on the SAR penetration depth and effective field size (EFS) has been studied for local hyperthermia. In this study, a 3-layered tissue model and a horn applicator radiating at 433 MHz has been used. The simulation results have been validated by comparison with results presented in the literature.

Numerical results demonstrate that increasing the thickness of water bolus leads to decreasing the maximum induced SAR. Also using distilled water for filling the water bolus results in increasing the SAR induced in the muscle layer.

The presented results show that the effect of water bolus thickness on the SAR penetration depth is negligible for both the fresh and distilled water.

For both the fresh and distilled water, by increasing the water bolus thickness, the elliptical EFS contours are converted to circular contours which may be more interested in local hyperthermia.

ACKNOWLEDGMENT

The authors thank Iran Telecommunication Research Center (ITRC) for financial support of this study.

REFERENCES

1. Wost, P., B. Hildebrandt, G. Sreenivasa, B. Rau, J. Gellermann, H. Riess, R. Felix, and P. M. Schlag, "Hyperthermia in combined treatment of cancer," *The LANCET Oncology*, Vol. 3, 487–497, 2002.
2. Juang, T., D. Neuman, J. Schlorff, and P. R. Stauffer, "Construction of a conformal water bolus vest applicator for hyperthermia treatment of superficial skin cancer," *IEEE Engineering in Medicine and Biology Society*, Vol. 2, 3467–3470, 2004.
3. Vorst, A. V., A. Rosen, and Y. Kotsuka, *RF/Microwave Interaction with Biological Tissues*, John Wiley, 2006.
4. Ibrahiem, A. and C. Dale, "Analysis of the temperature increase linked to the power induced by RF source," *Progress In Electromagnetics Research*, PIER 52, 23–46, 2005.
5. Siauve, N., L. Nicolas, C. Vollaire, A. Nicolas, and J. A. Vasconcelos, "Optimization of 3-D SAR distribution in local RF hyperthermia," *IEEE Trans. on Magnetics*, Vol. 40, No. 2, 1264–1267, 2004.
6. Samaras, T., P. J. M. Rietveld, and G. C. van-Rhoon, "Effectiveness of FDTD in predicting SAR distributions from the Lucite cone applicator," *IEEE Trans. on MTT*, Vol. 48, No. 9, 1522–1530, 2000.
7. Gupta, R. C. and S. P. Singh, "Analysis of the SAR distributions in three-layered bio-media in direct contact with a water-loaded modified box-horn applicator," *IEEE Trans. on MTT*, Vol. 53, No. 9, 2665–2671, 2005.
8. Lumöri, M. L. D., "Experimentally based modeling of field sources for tree-dimensional computation of SAR in electromagnetic hyperthermia and treatment planning," *IEEE Trans. on MTT*, Vol. 48, No. 9, 1522–1530, 2000.
9. Gupta, R. C. and S. P. Singh, "Elliptically bent slotted waveguide conformal focused array for hyperthermia treatment of tumors in curved region of human body," *Progress In Electromagnetics Research*, PIER 62, 107–125, 2006.

10. Gupta, R. C. and S. P. Singh, "Development and analysis of a microwave direct contact water-loaded box-horn applicator for therapeutic heating of bio-medium," *Progress In Electromagnetics Research*, PIER 62, 217–235, 2006.
11. Gelvich, E. A. and V. N. Mazokhin, "Resonance effects in applicator water boluses and their influence on SAR distribution patterns," *International Journal of Hyperthermia*, Vol. 16, 2000.
12. Neuman, D. G., P. R. Stauffer, S. Jacobsen, and F. Rossetto, "SAR pattern perturbations from resonance effects in water bolus layers used with superficial microwave hyperthermia applicators," *International Journal of Hyperthermia*, Vol. 18, 2002.
13. Gabriel, C., S. Gabriel, and E. Corthout, "The dielectric properties of biological tissues: I. Literature survey," *Phys. Med. Biol.*, Vol. 41, 2231–2249, 1996.
14. Gabriel, C., "Compilation of the dielectric properties of body tissues at RF and microwave frequencies," Brooks Air Force Base Tech. Rep. AL/OE-TR-1996-0037, Armstrong Lab., Brooks Air Force Base, TX, June 1996.
15. Jacobsen, D. G. and P. R. Stauffer, "Multifrequency radiometric determination of temperature profiles in a lossy homogeneous phantom using a dual-mode antenna with integral water bolus," *IEEE Trans. on MTT*, Vol. 50, No. 7, 1737–1746, 2002.
16. Maccarini, P. F., H. O. Rolfsnes, D. Neuman, and P. Stauffer, "Optimization of a dual concentric conductor antenna for superficial hyperthermia applications," *IEEE Engineering in Medicine and Biology Society*, Vol. 1, 2518–2521, 2004.
17. Deng, T., "Optimization of SAR distributions in liver and lung regions irradiated by the H-horn annular phased array hyperthermia system," *IEEE Trans. on MTT*, Vol. 39, No. 5, 852–856, 1991.